A MODEL FOR THE MECHANISM OF INCORPORATION OF Cu, Fe AND Zn IN THE STANNITE – KËSTERITE SERIES, Cu_2FeSnS_4 – Cu_2ZnSnS_4

Paola BONAZZI[§], Luca BINDI, Gian Piero BERNARDINI AND Silvio MENCHETTI

Dipartimento di Scienze della Terra, Università di Firenze, via La Pira 4, I-50121 Firenze, Italy

ABSTRACT

In order to clarify the symmetry problem along the stannite – kësterite join [Cu_2FeSnS_4 – Cu_2ZnSnS_4], a structural study of synthetic $Cu_2Fe_{1–x}Zn_xSnS_4$ single crystals was performed ($x = 0$, 0.2, 0.5, 0.7, 0.8 and 1, respectively). The metal distribution among the tetrahedral cavities was determined by refining different models in both the $I\bar{4}$ and $I\bar{4}2m$ space groups. The best agreement was obtained in $I\bar{4}2m$, even for the Zn-rich members of the series. However, two different mechanisms of incorporation take place along the stannite–kësterite join. For pure stannite and zincian stannite ($x = 0$, 0.2, 0.5), the $2a$ position (0,0,0) is mainly occupied by (Fe,Zn), whereas Cu is the dominant species at $4d$ (0,½,¼). For ferroan kësterite and pure kësterite ($x = 0.7$, 0.8, 1), the $2a$ position is fully occupied by Cu, whereas (Zn,Fe) and the remaining Cu are disordered at $4d$. On the basis of the structural results, pure *Me*–S bond-distances are proposed for Fe, Cu, Zn in both $2a$ and $4d$ sites, and the metal distribution among the tetrahedral sites is obtained accordingly. For $x \geq 0.7$, the *Me*–S distance found for the atom located at $2a$ closely approaches that found for the atom located at $4d$, thus producing a more regular framework. Accordingly, distortion parameters λ and σ^2 of the S(Me_3Sn) tetrahedron decrease with increasing Zn. This feature, in turn, is the reason for the pseudocubic symmetry of the lattice observed in the Zn-rich region ($2a$ close to the c parameter). The unit-cell volume linearly increases with increasing Zn, thus confirming the mainly covalent character of the bonds in these compounds. The previously noted inversion of slope in the unit-cell parameters at $x = 0.7$ corresponds to the point of the series wherein Cu becomes predominant at the $2a$ site. The proposed model accounts for the structural and geometrical variations observed along the stannite–kësterite series, even if no change of space group is assumed.

Keywords: stannite, kësterite, structure refinements, symmetry.

SOMMAIRE

Afin d'éclaicir le problème du changement de symétrie dans la solution solide entre stannite et kësterite [Cu_2FeSnS_4 – Cu_2ZnSnS_4], nous avons entrepris une étude structurale de monocristaux synthétiques de $Cu_2Fe_{1–x}Zn_xSnS_4$, $x = 0$, 0.2, 0.5, 0.7, 0.8 et 1, respectivement. Nous avons déterminé la distribution des atomes métalliques parmi les cavités tétraédriques par affinement de différents modèles dans les groupes spatiaux $I\bar{4}$ et $I\bar{4}2m$. La meilleure solution est celle que nous obtenons dans le groupe spatial $I\bar{4}2m$, même pour les membres riches en zinc de la série. Toutefois, deux mécanismes différents d'incorporation sont en opération le long de la série stannite–kësterite. Dans le cas de la stannite pure et de la stannite zincifère ($x = 0$, 0.2, 0.5), la position $2a$ (0,0,0) serait surtout remplie par (Fe,Zn), tandis que le Cu prédomine à la position $4d$ (0,½,¼). Dans le cas de la kësterite ferreuse et de la kësterite pure ($x = 0.7$, 0.8, 1), c'est la position $2a$ qui est remplie de Cu, tandis que (Zn,Fe) et le reste du Cu sont désordonnés à la position $4d$. A la lumière des résultats structuraux, nous proposons des longueurs de liaison *Me*–S idéales pour Fe, Cu, et Zn dans les sites $2a$ et $4d$, et nous obtenons ainsi la distribution des atomes métalliques sur les sites tétraédriques. Pour les compositions ayant $x \geq 0.7$, la distance *Me*–S pour l'atome situé au site $2a$ correspond à celle pour l'atome situé au site $4d$, ce qui mène à une trame plus régulière. Par conséquent, les indices de distorsion λ et σ^2 du tétraèdre S(Me_3Sn) diminuent à mesure qu'augmente la proportion de Zn. C'est en fait la raison de la symétrie pseudocubique du réseau observée sur l'intervalle de compositions riches en zinc ($2a$ se rapprochant du paramètre c). Le volume de la maille augmente de façon linéaire à mesure qu'augmente la proportion de zinc, ce qui confirme le caractère surtout covalent des liaisons dans ces composés. L'inversion dans la pente des paramètres à $x = 0.7$ qui avait été établie antérieurement correspond au point dans la série où le Cu devient prédominant au site $2a$. Notre modèle rend compte des variations structurales et géométriques le long de la série stannite–kësterite, sans même avoir à supposer un changement du groupe spatial.

(Traduit par la Rédaction)

Mots-clés: stannite, kësterite, affinement de la structure, symétrie.

---

§ *E-mail address*: pbcry@steno.geo.unifi.it

Introduction

The structures of stannite, Cu_2FeSnS_4, and kësterite, Cu_2ZnSnS_4, consist of a *ccp* array of sulfur atoms, with metal atoms occupying one half of the tetrahedral voids. The ordering of metal atoms leads to a sphalerite-derivative tetragonal unit-cell, with $a \approx a_{sph}$ and $c \approx 2a_{sph}$. However, owing to the presence of Sn, the packing of S atoms slightly deviates from ideality. According to Hall *et al.* (1978), the stannite and kësterite structures are topologically identical, but differ in the distribution of metal atoms, leading to different space-groups ($I\bar{4}2m$ for stannite and $I\bar{4}$ for kësterite, respectively). In this paper, we report the results of a structural study on synthetic crystals with chemical composition ranging from Cu_2FeSnS_4 to Cu_2ZnSnS_4.

Review of the Literature

The join between stannite, Cu_2FeSnS_4, and kësterite, Cu_2ZnSnS_4, has been the object of considerable study (Springer 1972, Hall *et al.* 1978, Kissin & Owens 1979, 1989, Kissin 1989, Corazza *et al.* 1986, Bernardini *et al.* 1990, 2000). Kissin & Owens (1979) proposed the existence of a miscibility gap between stannite and kësterite, supported by the discontinuity in the variation of the cell parameters as a function of Zn:Fe ratio. On the contrary, Corazza *et al.* (1986) proposed a continuous solid-solution on the basis of the cell-parameter trends determined by X-ray powder diffraction on several natural samples. Bernardini *et al.* (1990) reached the same conclusion in an investigation of the 750° and 550°C isotherms of the pseudobinary system $Cu_2Fe\ SnS_4$–Cu_2ZnSnS_4. According to Bernardini *et al.* (1990), homogeneous compounds were obtained with bulk compositions ranging from the Fe to the Zn end-member. An inversion of the trend of the unit-cell parameters was observed in the range 60–70 mole % Cu_2ZnSnS_4, thus suggesting a possible transition from $I\bar{4}2m$ to $I\bar{4}$ for the Zn-rich members. On the other hand, a new member of stannite-like composition was discovered by Kissin & Owens (1989) and named ferro-kësterite; according to these authors, the mineral differs from stannite in having the space group $I\bar{4}$. In their opinion, the weakly anisotropic mineral having a stannite-like composition previously described as *isostannite* (Claringbull & Hey 1955) could correspond to ferro-kësterite. The discreditation of *isostannite* was approved by IMA Commission on New Minerals and Mineral Names (Kissin & Owens 1989). A cubic polymorph of stannite, however, was documented during experimental investigations (Franz 1971, Wang 1982) by the powder-diffraction approach. Note that a cubic phase with $a \approx 2a_{sph}$ cannot easily be distinguished by powder-diffraction data from the pseudocubic ferrokësterite (Kissin & Owens 1989). The results recently obtained by Evstigneeva & Kabalov (2001) and Evstigneeva *et al.*

(2001) on the synthetic compound $Cu_{2-x}Fe_{1-x}SnS_4$ seem to confirm the existence of the cubic "prototype" of stannite ($a = 5.4179$ Å, space group $P\bar{4}3m$). According to these authors, the structure, determined by the Rietveld method, is characterized by a mixed population of Sn + Fe ($1a$) and Cu + Fe + Sn ($3c$). Lastly, an EPR and SQUID magnetometry study of synthetic end-members as well as natural samples did not provide evidence of the existence of distinct structural types for stannite and kësterite (Bernardini *et al.* 2000).

Experimental

Six single crystals of $Cu_2Fe_{1-x}Zn_xSnS_4$ ($x = 0, 0.2, 0.5, 0.7, 0.8$ and 1, respectively) were selected from the 750°C quenched run-products synthesized by Bernardini *et al.* (1990). In order to check the chemical composition of the investigated crystals, replicate analyses on different spots were carried out with a JEOL JXA 8600 electron microprobe. The crystals were found to be homogeneous within the analytical uncertainty. The chemical data are given in Table 1.

The unit-cell dimensions were determined by means of least-squares refinements using the same set of reflections ($36° < 2\theta < 54°$), measured with a CAD4 single-crystal diffractometer. In order to check the true symmetry, a redundant set of intensity data was collected for each crystal. In Table 2, we report the crystal data, together with the experimental details concerning the collection of data. Intensity data were subsequently reduced for Lorentz-polarization effects and corrected for absorption using the semi-empirical method of North *et al.* (1968) or, in the case of the crystal Fe*020*, with the empirical correction of Blessing (1995). Structure refinements were performed using the SHELXL-93 program (Sheldrick 1993). Scattering factors and anomalous dispersion terms were taken from the *International Tables for X-ray Crystallography*, volume IV (Ibers & Hamilton 1974). Tables of structure factors are available from the Depository of Unpublished Data, CISTI, National Research Council, Ottawa, Ontario K1A 0S2, Canada.

Symmetry

The two models proposed for the structure of these compounds by Hall *et al.* (1978) are based on different distributions of Cu, Zn, Fe atoms among the positions at (0,0,0), (0,½,¼) and (0,½,¾). In particular, the stannite structure is consistent with the $I\bar{4}2m$ symmetry, with Fe located at the origin ($2a$), and Cu at $4d$ (0,½,¼) (model I). On the other hand, in the kësterite structure, one Cu atom occupies the $2a$ (0,0,0) position, with Zn and the remaining Cu atom ordered at $2c$ (0,½,¼) and $2d$ (0,½,¾), respectively (model II). Owing to the different population at $2c$ and $2d$, the mirror plane parallel to (110) is lost (space group $I\bar{4}$). In both structural

TABLE 1. CHEMICAL COMPOSITION OF THE CRYSTALS INVESTIGATED ALONG THE JOIN STANNITE – KËSTERITE

	wt%	range	σ (%)	apfu	wt%	range	σ (%)	apfu	wt%	range	σ (%)	apfu
		Fe*100*				Fe*080*				Fe*050*		
Fe	12.77	12.61 – 12.80	0.06	0.99	10.02	9.92 – 10.15	0.07	0.78	6.63	6.59 – 6.70	0.07	0.52
Cu	29.52	29.45 – 29.60	0.05	2.01	29.21	29.13 – 29.31	0.05	2.00	28.78	28.70 – 28.90	0.05	1.98
Zn	–	–	–	–	3.17	3.08 – 3.21	0.11	0.21	7.46	7.38 – 7.52	0.09	0.50
Sn	28.25	28.19 – 28.34	0.05	1.03	28.37	28.26 – 28.44	0.05	1.04	27.96	27.88 – 28.00	0.05	1.03
S	29.35	29.30 – 29.39	0.07	3.97	29.30	29.19 – 29.39	0.06	3.97	29.05	28.97 – 29.12	0.06	3.97
total	99.89				100.07				99.88			
		Fe*030*				Fe*020*				Fe*000*		
Fe	3.93	3.87 – 3.97	0.10	0.31	2.77	2.65 – 2.81	0.11	0.22	–	–	--	--
Cu	28.75	28.68 – 28.82	0.05	1.99	28.55	28.48 – 28.61	0.05	1.98	28.41	28.38 – 28.54	0.05	1.98
Zn	10.54	10.44 – 10.59	0.07	0.71	12.24	12.21 – 12.34	0.07	0.82	14.78	14.71 – 14.87	0.07	1.00
Sn	27.80	27.71 – 27.90	0.05	1.03	27.58	27.52 – 27.68	0.05	1.02	28.09	27.92 – 28.15	0.06	1.05
S	28.87	28.79 – 28.94	0.06	3.96	28.81	28.78 – 28.88	0.06	3.96	28.65	28.54 – 28.71	0.06	3.96
total	99.89				99.96				99.93			

Note: Mean values calculated on at least four points, analyzed by electron microprobe; chemical formulae (*apfu*) on the basis of eight atoms.

TABLE 2. UNIT-CELL PARAMETERS AND EXPERIMENTAL DETAILS
OF INTENSITY-DATA COLLECTION FOR SIX CRYSTALS ON
THE JOIN STANNITE – KËSTERITE

|	Fe*100*	Fe*080*	Fe*050*	Fe*030*	Fe*020*	Fe*000*
a (Å)	5.4495(6)	5.446(4)	5.4329(3)	5.4250(6)	5.428(1)	5.434(1)
c (Å)	10.726(2)	10.757(8)	10.8235(8)	10.868(1)	10.864(1)	10.856(1)
V (Å^3)	318.53(8)	319.0(4)	319.47(3)	319.85(6)	320.09(9)	320.56(9)
crystal size (μm)	110x120x200	80x100x100	120x120x150	110x110x120	20x60x80	160x180x230
instrument	CAD4	CAD4	CAD4	CAD4	K/CCD	CAD4
scan mode	ω-2θ	ω-2θ	ω-2θ	ω-2θ	ω/φ	ω-2θ
scan width (°)	1.20	1.30	1.20	1.30	2.0*	1.40
scan speed	3.3 °/min	2.7 °/min	3.3 °/min	2.7 °/min	280 s/frame	3.3 °/min
2θ $_{max}$ (MoKα)	100	90	100	100	101	100
range of h,k,l	0 → 11	0 → 10	0 → 11	0 → 11	-11 → 11	0 → 11
	0 → 11	0 → 10	0 → 11	0 → 11	-11 → 11	0 → 11
	-23 → 23	-21 → 21	-23 → 23	-23 → 23	-12 → 23	-23 → 23
n. measured refl.	1873	1495	1878	1880	2024	1880
R_{symm} ($I\bar{4}$)	3.02	3.59	4.78	2.50	5.24	4.36
n. unique refl.	867	686	869	866	732	866
n. observed refl.	867	648	858	835	653	861
(Fo>4σ (Fo))						
R_{symm} ($I\bar{4}2m$)	3.34	4.43	5.17	3.13	5.78	5.13
n. unique refl.	528	423	530	528	491	528
n. observed refl.	528	410	527	519	433	525
(Fo>4σ (Fo))						

* rotation per frame
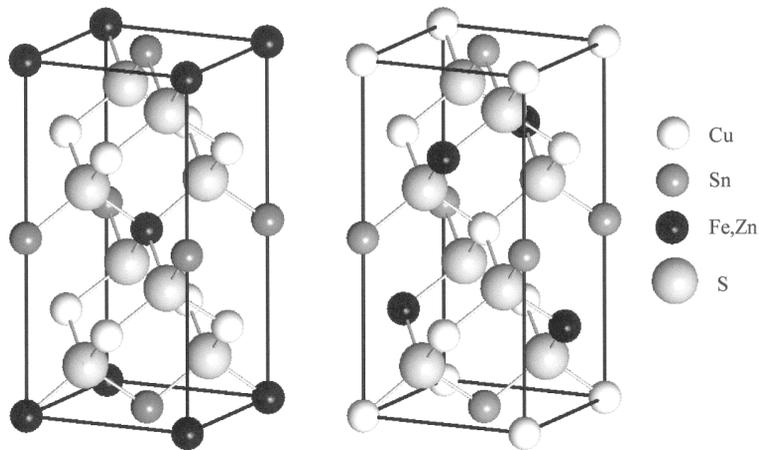
FIG. 1.   Structural models I (left) and II (right) for stannite and kësterite (after Hall *et al.* 1978).

TABLE 3. RESULTS OF PRELIMINARY REFINEMENTS IN THE SPACE GROUP $I\bar{4}$
FOR SIX CRYSTALS ON THE JOIN STANNITE – KËSTERITE

model	A	B	C	D
Fe100	$2a$ = Fe $2c$ = Cu $2d$ = Cu R_{obs} = 2.01 R_{all} = 2.02			$2a$ = Cu $2c$ = Fe $2d$ = Cu non-convergent
Fe080	$2a$ = 0.8 Fe + 0.2 Zn $2c$ = Cu $2d$ = Cu R_{obs} = 3.00 R_{all} = 3.22	$2a$ = 0.8 Fe + 0.2 Cu $2c$ = 0.8 Cu + 0.2 Zn $2d$ = Cu R_{obs} = 3.09 R_{all} = 3.29	$2a$ = 0.8 Cu + 0.2 Zn $2c$ = 0.8 Fe + 0.2 Cu $2d$ = Cu non-convergent	$2a$ = Cu $2c$ = 0.8 Fe + 0.2 Zn $2d$ = Cu non-convergent
Fe050	$2a$ = 0.5 Fe + 0.5 Zn $2c$ = Cu $2d$ = Cu R_{obs} = 2.65 R_{all} = 2.68	$2a$ = 0.5 Fe + 0.5 Cu $2c$ = 0.5 Cu + 0.5 Zn $2d$ = Cu R_{obs} = 2.80 R_{all} = 2.83	$2a$ = 0.5 Cu + 0.5 Zn $2c$ = 0.5 Fe + 0.5 Cu $2d$ = Cu R_{obs} = 3.49 R_{all} = 3.56	$2a$ = Cu $2c$ = 0.5 Fe + 0.5 Zn $2d$ = Cu R_{obs} = 3.11 R_{all} = 3.17
Fe030	$2a$ = 0.3 Fe + 0.7 Zn $2c$ = Cu $2d$ = Cu R_{obs} = 2.72 R_{all} = 2.85	$2a$ = 0.3 Fe + 0.7 Cu $2c$ = 0.3 Cu + 0.7 Zn $2d$ = Cu R_{obs} = 2.92 R_{all} = 3.03	$2a$ = 0.3 Cu + 0.7 Zn $2c$ = 0.3 Fe + 0.7 Cu $2d$ = Cu R_{obs} = 3.06 R_{all} = 3.24	$2a$ = Cu $2c$ = 0.3 Fe + 0.7 Zn $2d$ = Cu R_{obs} = 2.66 R_{all} = 2.79
Fe020	$2a$ = 0.2 Fe + 0.8 Zn $2c$ = Cu $2d$ = Cu R_{obs} = 3.81 R_{all} = 4.58	$2a$ = 0.2 Fe + 0.8 Cu $2c$ = 0.2 Cu + 0.8 Zn $2d$ = Cu R_{obs} = 4.07 R_{all} = 4.83	$2a$ = 0.2 Cu + 0.8 Zn $2c$ = 0.2 Fe + 0.8 Cu $2d$ = Cu R_{obs} = 4.33 R_{all} = 5.16	$2a$ = Cu $2c$ = 0.2 Fe + 0.8 Zn $2d$ = Cu R_{obs} = 3.77 R_{all} = 4.53
Fe000	$2a$ = Zn $2c$ = Cu $2d$ = Cu R_{obs} = 3.80 R_{all} = 3.83			$2a$ = Cu $2c$ = Zn $2d$ = Cu R_{obs} = 3.41 R_{all} = 3.47

models, Sn is located at 2b $(0,0,\frac{1}{2})$; S lies on the (110) mirror plane at 8i (x,x,z) (model I) or at the general position 8g (x,y,z) (model II) (Fig. 1).

In order to determine the distribution of metal atoms without symmetry constraints, the structure was preliminarily refined in the $I\bar{4}$ space group following the site-assignment schemes reported in Table 3. From the results, there is clear evidence for two distinct mechanisms of substitution along the stannite–kësterite join. For pure stannite and zincian stannite $(x = 0, 0.2, 0.5)$, the better agreement is obtained with Fe, Zn at the 2a position (column A, Table 3). For ferroan kësterite and pure kësterite $(x = 0.7, 0.8, 1)$, the better agreement is obtained with Cu at 2a (column D, Table 3). However, a careful examination of the structural details [i.e., $x(S) = y$ (S); $U_{11}(S) = U_{22}$ (S)] reveals the symmetry to be consistent with the $I\bar{4}2m$ space group within the limits of experimental errors, even for the Zn-rich crystals. For this reason, all the structure refinements were repeated in $I\bar{4}2m$. The distributions of metal atoms reported in Table 3 (A, B, C, D) were modified according to the higher symmetry (E, F, G, H, respectively), by changing the positions of the metal atoms from 2c and 2d ($I\bar{4}$) into 4d ($I\bar{4}2m$). As expected, for $x = 0, 0.2$ and 0.5, we obtained a better R index with Fe, Zn at 2a $(0,0,0)$ and Cu at 4d $(0,\frac{1}{2},\frac{1}{4})$; for $x = 0.7, 0.8$ and 1, the lower values of R were achieved with Cu at 2a $(0,0,0)$ and Cu, Zn, Fe at 4d $(0,\frac{1}{2},\frac{1}{4})$. Site occupancies were fixed during the structure refinements. It is noteworthy that the R values obtained in the $I\bar{4}2m$ symmetry (Table 4) are lower than those obtained in $I\bar{4}$ also for kësterite, thus suggesting a disordered distribution of Cu, Zn and Fe at 4d. In Figure 2, we report the normalized values $|R|_{E,H} = R_{E,H} / (R_E + R_H)$ obtained in $I\bar{4}2m$ for a model with Fe,Zn at 2a (model E) and with Cu at 2a (model H), respectively, as a function of the Zn content. It clearly appears that the improvement of model E with respect

to model H becomes gradually poorer as the Zn content increases. As for compositions with $x = 0.7$ and 0.8, models E and H become nearly equivalent, because the mean number of electrons for 0.75 Zn + 0.25 Fe equals that of Cu. Values of R indices corresponding to the final models are given in Table 4, together with coordinates, isotropic displacement parameters and site scattering.
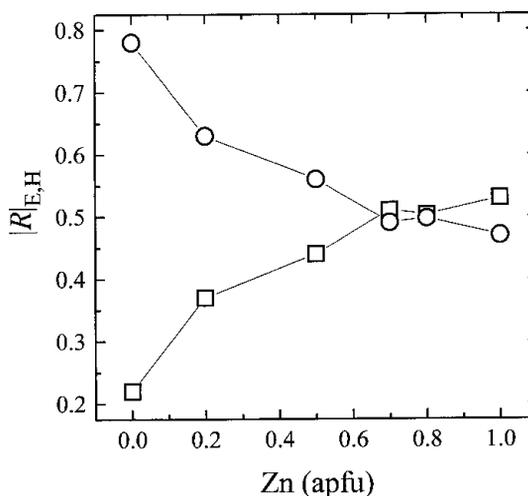

FIG. 2. Normalized values $|R|_{E,H} = R_{E,H} / (R_E + R_H)$ obtained in $I\bar{4}2m$ for the model E and H plotted against Zn content. The empty squares and empty circles correspond to $|R|_E$ (Fe,Zn at 2a) and $|R|_H$ (Cu at 2a), respectively.

TABLE 4. ATOM PARAMETERS OF THE FINAL MODELS (SPACE GROUP $I\bar{4}2m$), TOGETHER WITH THE CORRESPONDING R INDICES FOR SIX CRYSTALS ON THE JOIN STANNITE – KËSTERITE

	Fe100	Fe080	Fe050	Fe030	Fe020	Fe000
x (S)	.75581(5)	.75528(9)	.75545(7)	.75621(6)	.75611(7)	.75617(8)
z (S)	.87012(3)	.87028(6)	.87072(4)	.87185(4)	.87184(4)	.87208(5)
U_{eq} (2a)	.01219(6)	.01227(11)	.01481(8)	.01734(8)	.01969(11)	.01516(11)
U_{eq} (2b)	.01025(4)	.00987(8)	.01079(6)	.00985(5)	.01328(9)	.00711(7)
U_{eq} (4d)	.01924(6)	.01865(10)	.01843(7)	.01558(6)	.01781(9)	.01300(8)
U_{eq} (8i)	.01134(8)	.01100(11)	.01123(8)	.01030(8)	.01236(14)	.00775(11)
s.s. (2a)	26.0	26.8	28.0	29.0	29.0	29.0
s.s. (2b)	50.0	50.0	50.0	50.0	50.0	50.0
s.s. (4d)	29.0	29.0	29.0	28.9	29.1	29.5
s.s. (8i)	16.0	16.0	16.0	16.0	16.0	16.0
R_{obs}(%)	1.30	2.32	2.22	2.03	3.73	2.90
R_{all}(%)	1.30	2.36	2.23	2.04	4.52	2.92

Note: s.s. = site scattering fixed during the structure refinements

METAL DISTRIBUTION AND BOND DISTANCES

In view of the difficulties in speculating on bond distances in terms of geometrical criteria in non-ionic compounds, we can only tentatively compare the relative variations as a function of the variation in chemical composition.

An apparent unusual feature is the difference between the value of the Cu–S distance at $4d$ $(0,\frac{1}{2},\frac{1}{4})$ for the Fe100 crystal (2.318 Å) and that at $2a$ $(0,0,0)$ for the Fe000 crystal (2.332 Å). It is reasonable to attribute this difference to the presence of the relatively large Sn atom, which occupies half of the tetrahedral cavities at $z = 0$, $\frac{1}{2}$. Owing to symmetry constraints, in fact, the position along the **c** axis of the unique sulfur atom depends on the cation population at the $z = 0$, $\frac{1}{2}$ layer as well as that at the $z = \frac{1}{4}$, $\frac{3}{4}$ layer. Therefore, the Me–S distances (Me = Fe, Zn, or Cu) in the tetrahedra located at $z = 0$, $\frac{1}{2}$ are affected by the presence of Sn at the same level. This accounts for the unusual value of the Fe–S distance in Fe100 (2.341 Å) which, as already pointed out by Hall *et al.* (1978), is much longer than those observed for Fe–S in chalcopyrite-type minerals (Hall 1975). The distance between adjacent layers of sulfur atoms along [001] is plotted in Figure 3. As expected, along the entire compositional range, the thickness of the layer at $z = 0$, $\frac{1}{2}$ is much greater than that of the layer at $z = \frac{1}{4}$, $\frac{3}{4}$. For this reason, in order to obtain the metal distribution among the tetrahedral sites, distances belonging to different positions cannot be compared. The "pure" Me–S distances were assumed to have the following values: [Fe–S]$_{2a}$ = 2.341 Å and [Cu–S]$_{4d}$ = 2.318 Å from the refinement of Fe100; [Cu–S]$_{2a}$ = 2.332 Å from the refinement of Fe000; [Zn–S]$_{4d}$ = 2.350 Å was extrapolated assuming an atomic population of 0.5 Zn + 0.5 Cu at $4d$ $(0,\frac{1}{2},\frac{1}{4})$ in Fe000. Taking into account the observed difference Δ(Fe$_{2a}$ – Cu$_{2a}$) = 0.009 Å and Δ(Zn$_{4d}$ – Cu$_{4d}$) = 0.032 Å, the following pure Me–S distances were tentatively assumed: [Fe–S]$_{4d}$ = 2.327 Å and [Zn–S]$_{2a}$ = 2.364 Å. The site population for $2a$ and $4d$ positions reported in Table 5 was obtained on the basis of the mean number of electrons (Table 4), using the pure Me–S distances. Theoretical distances (Me–S$_{calc}$) were then calculated accordingly (Table 5). As shown in Figure 4, a satisfactory agreement between the theoretical and observed distances in the Me–S tetrahedron is obtained (r = 0.998) along the entire compositional range. For $x \geq 0.7$, the distance found for the Me atom located at $2a$ position closely approaches that found for the atom located at $4d$ position, thus producing a more homogeneous set of Me–S distances. As a consequence, the distortion parameters λ and σ^2 of the S(Me_3Sn) tetrahedron decrease with increasing Zn content (Fig. 5). The $2b$ position was assumed to be occupied by Sn alone for all crystals examined, in spite of the slight gradual variation of the Sn–S distance over the interval from 2.414 to 2.409 Å.
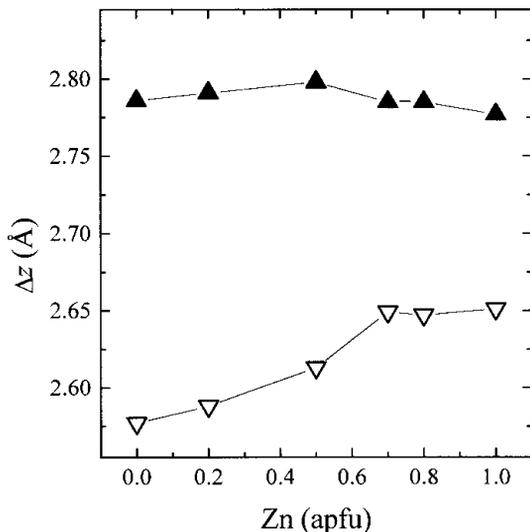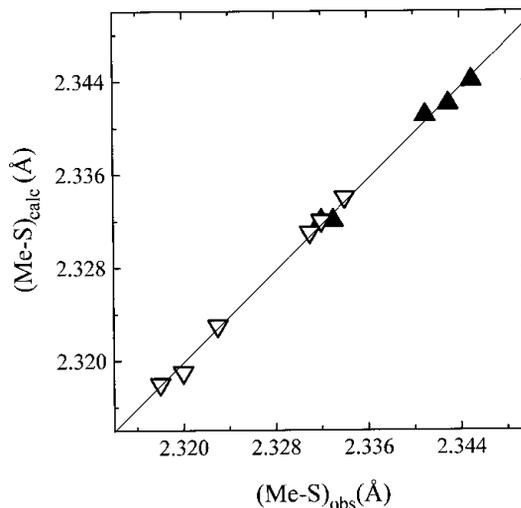

FIG. 3.   Distances between adjacent sulfur layers along [001] plotted against Zn content. The solid upward triangles and the empty downward triangles refer to the layers at $z = 0$, $\frac{1}{2}$ and at $z = \frac{1}{4}$, $\frac{3}{4}$, respectively.

FIG. 4.   Calculated *versus* observed Me–S distance for metals at $2a$ (solid upward triangles) and $4d$ (empty downward triangles). The equation of the regression line is: y = 0.98x + 0.038 (r = 0.998).

TABLE 5. SELECTED BOND-DISTANCES (Å) AND ANGLES (°), TOGETHER WITH THE ESTIMATED
SITE-POPULATIONS, FOR SIX CRYSTALS ON THE JOIN STANNITE – KËSTERITE

	Fe100	Fe080	Fe050	Fe030	Fe020	Fe000
(2a)						
s. p.	$Fe_{1.00}$	$Fe_{0.78}Zn_{0.14}Cu_{0.08}$	$Fe_{0.40}Zn_{0.20}Cu_{0.40}$	$Cu_{1.00}$	$Cu_{1.00}$	$Cu_{1.00}$
$(Me-S)_{obs}$ (x4)	2.341(1)	2.345(1)	2.343(1)	2.332(1)	2.333(1)	2.332(1)
S-Me-S (x4)	110.73(1)	110.74(3)	110.90(1)	110.90(1)	110.86(1)	110.76(2)
S-Mc-S (x2)	106.98(2)	106.97(7)	106.65(2)	106.66(3)	106.72(3)	106.92(3)
σ^2	3.757	3.778	4.819	4.798	4.566	3.953
$(Me-S)_{calc}$	2.341	2.344	2.342	2.332	2.332	2.332
(2b)						
s. p.	$Sn_{1.00}$	$Sn_{1.00}$	$Sn_{1.00}$	$Sn_{1.00}$	$Sn_{1.00}$	$Sn_{1.00}$
$(Me-S)_{obs}$ (x4)	2.414(1)	2.411(2)	2.410(1)	2.409(1)	2.409(1)	2.409(1)
S-Me-S (x4)	109.45(1)	109.57(3)	109.69(1)	109.53(1)	109.51(1)	109.41(1)
S-Mc-S (x2)	109.51(2)	109.27(7)	109.03(2)	109.36(2)	109.39(3)	109.60(3)
σ^2	0.001	0.024	0.118	0.007	0.004	0.010
(4d)						
s. p.	$Cu_{2.00}$	$Fe_{0.02}Zn_{0.06}Cu_{1.92}$	$Fe_{0.10}Zn_{0.30}Cu_{1.60}$	$Fe_{0.30}Zn_{0.70}Cu_{1.00}$	$Fe_{0.20}Zn_{0.80}Cu_{1.00}$	$Zn_{1.00}Cu_{1.00}$
$(Me-S)_{obs}$ (x4)	2.318(1)	2.320(1)	2.323(1)	2.331(1)	2.332(1)	2.334(1)
S-Me-S (x4)	107.99(1)	108.12(3)	108.44(1)	108.82(1)	108.80(1)	108.80(1)
S-Mc-S (x2)	112.47(2)	112.21(6)	111.56(2)	110.77(2)	110.82(2)	110.82(2)
σ^2	5.352	4.468	2.607	1.011	1.095	1.084
$(Me-S)_{calc}$	2.318	2.319	2.323	2.331	2.332	2.334

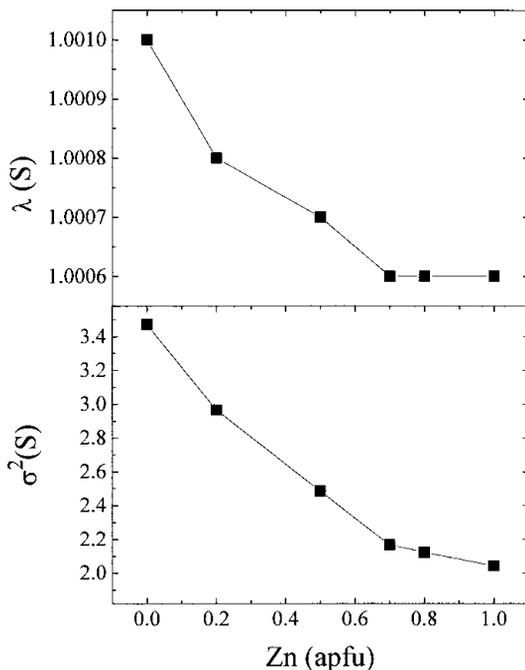Note: the angle variance σ^2 was computed according to Robinson *et al.* (1971)

FIG. 5. Distortion parameters of the $S(Me_3Sn)$ tetrahedron plotted against Zn content. Quadratic elongation (λ) and angle variance σ^2 were computed according to Robinson *et al.* (1971).

CONCLUDING REMARKS

As shown in Figure 6, the unit-cell volume increases linearly with increasing Zn content, in atoms per formula unit, *apfu* [vol ($Å^3$) = 318.56(5) + 1.94(9) (Zn_{apfu}), r = 0.996], which confirms the mainly covalent character of the chemical bond in these compounds (ionic radii: Fe > Zn). The previously noted inversion of slope in the unit-cell parameter plot at $x = 0.7$ (Fig. 6) corresponds to the point in the series at which Cu becomes dominant at the 2a site. The combined entry of the smaller atom (Cu) in the larger tetrahedron (2a), and the increase in the proportion of the larger atom (Zn) in the smaller tetrahedron (4d), causes the mean *Me*–S distances in the (2a) and (4d) tetrahedra to converge toward a common value (Fig. 7). This feature, in turn, is the reason for the pseudocubic symmetry of the structure observed in the Zn-rich region (2a close to c). According to Kissin & Owens (1979), the discontinuity in the cell-parameter plot supports the hypothesis that stannite and kësterite crystallize in two different space-groups. On the contrary, we contend that the "pure" bond distances for Fe, Cu, and Zn in both 2a and 4d sites account well for the structural and geometrical variations observed along the stannite–kësterite series, even if no change in the space group ($I\bar{4}2m$) is assumed. Although we cannot exclude the possibility that minerals of the Cu_2FeSnS_4 – Cu_2ZnSnS_4 series can crystallize in different space-groups in nature, we believe that
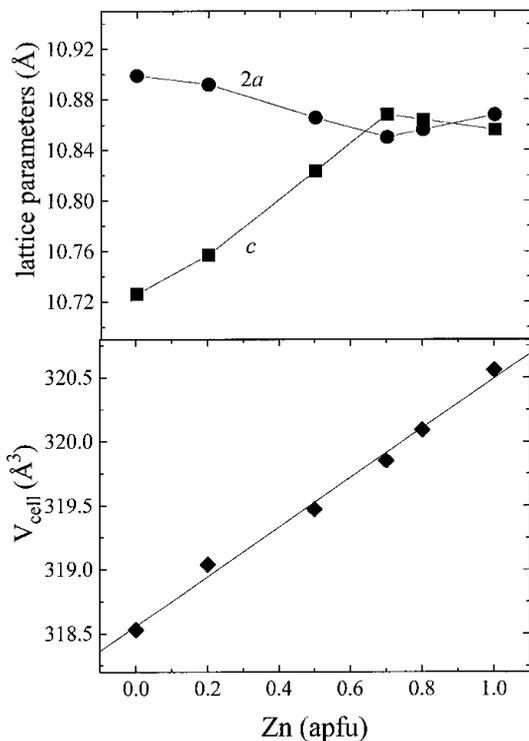
FIG. 6. Variation of the lattice parameters (*2a*: circles, *c*: squares) and the unit-cell volume (diamonds) as a function of Zn content.
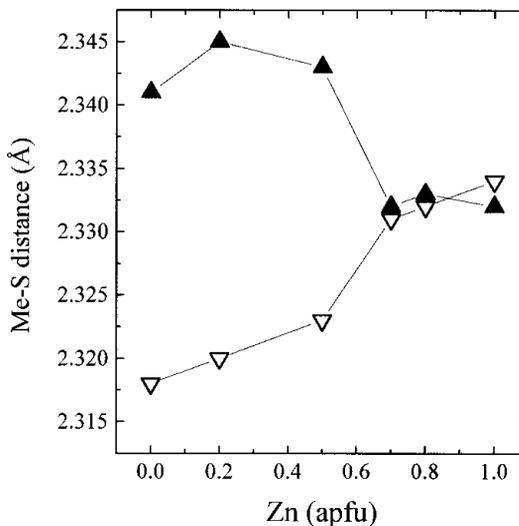

FIG. 7. *Me*–S bond distances plotted against Zn content. The solid upward triangles and the empty downward triangles refer to the metal atoms located at *2a* and at *4d*, respectively.

a discontinuity in the trend of the cell parameters does not necessarily imply a change in space group.

REFERENCES

BERNARDINI, G.P., BONAZZI, P., CORAZZA, M., CORSINI, F., MAZZETTI, G., POGGI, L. & TANELLI, G. (1990): New data on the Cu_2FeSnS_4 – Cu_2ZnSnS_4 pseudobinary system at 750 and 550°C. *Eur. J. Mineral.* **2**, 219-225.

_____, BORRINI, D., CANESCHI, A., DI BENEDETTO, F., GATTESCHI, D., RISTORI, S. & ROMANELLI, M. (2000): EPR and SQUID magnetometry study of Cu_2FeSnS_4 (stannite) and Cu_2ZnSnS_4 (kesterite). *Phys. Chem. Minerals* **27**, 453-461.

BLESSING, R.H. (1995): An empirical correction for absorption anisotropy. *Acta Crystallogr.* **A51**, 33-38.

CLARINGBULL, G.F. & HEY, M.H. (1955): Stannite and isostannite. *Mineral. Soc.*, *Notice* **91**(2). (see *Mineral. Abstr.* **13**, 31, 1956).

CORAZZA, M., CORSINI, F. & TANELLI, G. (1986): Stannite group minerals: investigations on stannite and kesterite. *Rend. Soc. Ital. Mineral. Petrol.* **41**(2), 217-222.

EVSTIGNEEVA, T.L. & KABALOV, YU.K. (2001): Crystal structure of the cubic modification of Cu_2FeSnS_4. *Kristallografiya* **46**(3), 418-422 (in Russ.).

_____, RUSAKOV, V.S., BURKOVSKY, I.A. & KABALOV, YU.K. (2001): New data on the isomorphism Cu–Fe in sulphides of stannite family. *In* Mineral Deposits at the Beginning of the 21st Century (Piestrzynski *et al.*, eds) Zwets & Zeitlinger, Lisse, The Netherlands (1075-1078).

FRANZ, E.D. (1971): Kubischer Zinnkies und tetragonaler Zinnkies mit Kupferkiesstruktur. *Neues Jahrb. Mineral., Monatsh.*, 218-223.

HALL, S.R. (1975): Crystal structures of the chalcopyrite series. *Can. Mineral.* **13**, 168-172.

_____, SZYMAŃSKI, J.T. & STEWART, J.M. (1978): Kesterite, $Cu_2(Zn,Fe)SnS_4$, and stannite, $Cu_2(Fe,Zn)SnS_4$, structurally similar but distinct minerals. *Can. Mineral.* **16**, 131-137.

IBERS, J.A. & HAMILTON, W.C., eds. (1974) *International Tables for X-ray Crystallography* IV. The Kynoch Press, Birmingham, U.K.

KISSIN, S.A. (1989): A reinvestigation of the stannite (Cu_2FeSnS_4) – kesterite (Cu_2ZnSnS_4) pseudobinary system. *Can. Mineral.* **27**, 689-697.

_____ & OWENS, D.R. (1979): New data on stannite and related tin sulfide minerals. *Can. Mineral.* **17**, 125-135.

_____ & _____ (1989): The relatives of stannite in the light of new data. *Can. Mineral.* **27**, 673-688.

NORTH, A.C.T., PHILLIPS, D.C. & MATHEWS, F.S. (1968): A semiempirical method of absorption correction. *Acta Crystallogr.* **A24**, 351-359.

ROBINSON, K., GIBBS, G.V. & RIBBE, P.H. (1971): Quadratic elongation; a quantitative measure of distortion in coordination polyhedra. *Science* **172**, 567-570.

SHELDRICK, G.M. (1993): *SHELXL-93: a New Structure Refinement Program*. University of Göttingen, Göttingen, Germany.

SPRINGER, G. (1972): The pseudobinary system Cu_2FeSnS_4 – Cu_2FeSnS_4 and its mineralogical significance. *Can. Mineral.* **11**, 535-541.

WANG, N. (1982): A contribution to the stannite problem. *In* Ore Genesis – The State of the Art (G.C. Amstutz, A. El Goresy, G. Frenzel, C. Kluth, G. Moh, A. Wauschkuhn & R.A. Zimmermann, eds.). Springer-Verlag, Berlin, Germany.